Supporting Information

for

Manganese(II) Reconstituted and Native Toluene/*o*-xylene Monooxygenase Hydroxylase X-ray Crystal Structures Reveal Rotamer Shifts in Conserved Residues and an Enhanced View of the Protein Interior

Michael S. McCormick, Matthew H. Sazinsky, Karen L. Condon, and Stephen J. Lippard*
Department of Chemistry, Massachusetts Institute of Technology, Cambridge, Massachusetts 02139

Preparation of apo ToMOH. ToMOH was expressed and purified as previously described,[1] except that thioglycolate was not included in the purification buffers. Apo ToMOH was prepared as previously described for MMOH,[2] with slight modifications as described below. A 2.8 mL solution of 50 μM ToMOH, 4 mM 1,10-phenanthroline, 1 mM methyl viologen, 100 mM NaCl, 5% (v/v) glycerol, and 25 mM MOPS at pH 7.0 was degassed by repeated vacuum purge /N_2 backfill cycles. A 20 μL aliquot of 400 mM sodium dithionite was added to the ToMOH solution in an anaerobic chamber and the solution was incubated overnight at 4 °C. Apo protein was separated from the iron extraction reagents with an EconoPac 10DG (Bio-Rad) desalting column and contained 0.03 ± 0.01 Fe atoms per ToMOH dimer as determined by the ferrozine assay.[3]

Crystallization. Crystallization of Mn(II)-ToMOH was accomplished by the hanging drop vapor diffusion method at 20 °C, with slight modification of the previously described conditions,[1] as described below. Precipitant solution contained 100 mM HEPES at pH 7.5, 2.1 - 2.5 M $(NH_4)_2SO_4$, 2-4 % (v/v) polyethylene glycol 400, and 10 or 20 mM $MnCl_2{\cdot}4H_2O$. Hanging drops contained 2 μL 50 μM apo ToMOH in 10 mM MES, 10% (v/v) glycerol, pH 7.1 buffer, 1 μL precipitant solution, and 1 μL microseed stock solution (native ToMOH microcrystals in 100 mM HEPES at pH 7.5, 2.3 M $(NH_4)_2SO_4$, 2% (v/v) polyethylene glycol 400 buffer). Microseeds of the native protein insignificantly comprise less than 0.1% of the final diffraction data set. Crystals did not form in the absence of $MnCl_2$, suggesting that active site metals stabilize ToMOH. Crystals of native ToMOH

were grown using conditions identical to those employed in obtaining Mn(II)-ToMOH crystals, with exception that $MnCl_2 \cdot 4H_2O$ was not present in the crystallization buffer, and the incubation temperature was 18 °C instead of 20 °C.

Crystal Annealing. Crystal annealing was conducted at the Stanford Synchrotron Radiation Laboratory (SSRL) on beam line 9-2 directly before data collection. Utilizing the flow control feature within the SSRL BLU-ICE[4] data collection software suite, native ToMOH crystals were subject to 5 s annealing times directly before and after irradiating with 10 s 12.7 keV X-ray pulse. The crystal used to obtain the native ToMOH data reported here saw the most dramatic increase in resolution, from 2.55 Å to 1.85 Å following one round of annealing. Using a cryo pin mounted thermocouple, analysis of this procedure indicated that the crystal temperature increases from 100 to 233 K before returning to 100 K during a 5 s annealing time period.

Data Collection and Refinement. Mn(II)-ToMOH X-ray diffraction data were collected at SSRL on beam line 9-2 at 100 K. Data were indexed, integrated, and scaled by using the HKL 2000 software suite,[5] and initial phases were determined by rigid body refinement molecular replacement in CNS.[6] Molecular replacement was conducted in CNS using the fully refined native ToMOH coordinates (PDB code 1T0Q) with coordinating ligand side chains and all non-protein atoms removed as a starting model. Subsequent models were built in XtalView[7] and refined using CNS. Data collection and refinement statistics can be found in Table S1**.**

X-ray diffraction data on native ToMOH were similarly collected at SSRL on BL 9-2 at 101K. Data were indexed, integrated, and scaled by using the HKL 2000 software suite. Phasing of the native ToMOH data was accomplished by using EPMR[8] and ToMOH coordinates (PDB code 1T0Q) in which all non-protein atoms and the side chains of the coordinating ligands and residues I100, T201, N202, Q228, and S232 removed as a starting model. Subsequent models were built in Coot[9] and refined using REFMAC5[10] in CCP4.[11] MSDchem ideal coordinates, CNS parameters, and CNS topology files for the polyethylene glycol component (residue name P6G) were obtained from the HIC-Up database.[12]

Statistical and geometrical analyses of Mn(II)-ToMOH and 1.85 Å $ToMOH_{ox}$ using PROCHECK[13] indicated that 99.8% of the residues in each structure occupied allowed regions of their respective Ramachandran plots. The complete data collection and refinement statistics can be found in Table S1**.**

Table S1. Data Collection and Refinement Statistics.

	$ToMOH_{ox}$	Mn(II)-ToMOH
Data Collection		
Beamline	SSRL 9-2	SSRL 9-2
Wavelength (Å)	0.979	0.979
Space Group	$P3_121$	$P3_121$
Unit Cell Dimensions (Å)	182.6 x 182.6 x 68.1	182.5 x 182.5 x 67.8
Resolution Range (Å)	50 - 1.85	30 - 2.20
Total Reflections	1,064,847	385,987
Unique Reflections	99,695	64,565
Completeness (%)[a]	90.4 (78.9)	98.0 (91.9)
$I/\sigma(I)$[a]	55.8 (5.5)	17.5 (4.5)
R_{sym} (%)[a,b]	8.7 (43.0)	6.9 (43.1)
Phasing Method	Molecular Replacement	Molecular Replacement
Refinement		
R_{cryst} (%)[c]	19.5	21.5
R_{free} (%)[d]	22.9	24.4
No. Protein Atoms	7335	7346
No. Non-Protein Atoms	421	201
R.m.s Deviation Bond Length (Å)	0.018	0.007
R.m.s Deviation Bond Angles (deg)	1.70	1.26
Average B-value ($Å^2$)	41.8	50.8

[a]Values in parentheses are for the highest resolution shell. [b]$R_{sym} = \Sigma_i\Sigma_{hkl}|I_i(hkl) - \langle I(hkl)\rangle|/ \Sigma_{hkl}\langle I(hkl)\rangle$, where $I_i(hkl)$ is the ith measured diffraction intensity and $\langle I(hkl)\rangle$ is the mean intensity for the Miller index (hkl). [c]$R_{cryst} = \Sigma_{hkl}||F_o(hkl)| - |F_c(hkl)||/ \Sigma_{hkl}|F_o(hkl)|$. [d]$R_{free} = R_{cryst}$ for a test set of reflections (5% in each case).

Table S2. Ångstrom distances between atoms and ions in the active sites of 2.15 Å $ToMOH_{ox}$ (PDB code 1T0Q), 1.85 Å $ToMOH_{ox}$, 1.96 Å $MMOH_{ox}$ (PDB code 1FZ1), and 1.70 Å $MMOH_{ox}$ (PDB code 1MTY).

2.15 Å ToMOHox			1.85 Å ToMOHox			1.96 Å MMOHox			1.70 Å MMOHox		
Atom	Atom	Dist.	Atom	Atom	Dist.	Atom	Atom	Dist.	Atom	Atom	Dist.
Fe1	Fe2	3.1	Fe1	Fe2	3.1	Fe1	Fe2	3.2	Fe1	Fe2	3.1
Fe1	E104 OE1	2.2	Fe1	E104 OE1	2.1	Fe1	E114 OE1	2.0	Fe1	E114 OE1	1.9
Fe1	H137 ND1	2.1	Fe1	H137 ND1	2.3	Fe1	H147 ND1	2.2	Fe1	H147 ND1	2.1
Fe1	E134 OE2	2.1	Fe1	E134 OE2	2.2	Fe1	E144 OE2	2.2	Fe1	E144 OE2	2.1
Fe1	μOH1	2.2	Fe1	μOH1	2.1	Fe1	μOH1	1.8	Fe1	μOH1	1.7
Fe1	μOH2	2.2	Fe1	μOH2	2.4	Fe1	μOH2	2.7	Fe1	μOH2	2.3
Fe1	H2O1	2.0	Fe1	H2O1	2.3	Fe1	H2O1	2.4	Fe1	H2O1	2.3
Fe2	E197 OE2	1.9	Fe2	E197 OE2	1.8	Fe2	E209 OE2	2.2	Fe2	E209 OE2	1.9
Fe2	H234 ND1	2.2	Fe2	H234 ND1	2.2	Fe2	H246 ND1	2.2	Fe2	H246 ND1	2.2
Fe2	E231 OE1	2.3	Fe2	E231 OE1	2.2	Fe2	E243 OE1	2.3	Fe2	E243 OE1	2.0
Fe2	E134 OE1	2.2	Fe2	E134 OE1	2.1	Fe2	E144 OE1	2.5	Fe2	E144 OE1	2.5
Fe2	μOH-TG*	2.0	Fe2	μOH1	1.8	Fe2	μOH1	2.0	Fe2	μOH1	2.0
Fe2	μOH2	2.1	Fe2	μOH2	2.3	Fe2	μOH2	2.8	Fe2	μOH2	2.5
μOH1	E231 OE2	2.3	μOH1	E231 OE2	2.4	μOH1	E243 OE2	2.8	μOH1	E243 OE2	2.7
H2O1	E104 OE2	2.5	H2O1	E104 OE2	2.7	H2O1	E114 OE2	2.6	H2O1	E114 OE2	2.8

*Thioglycolate

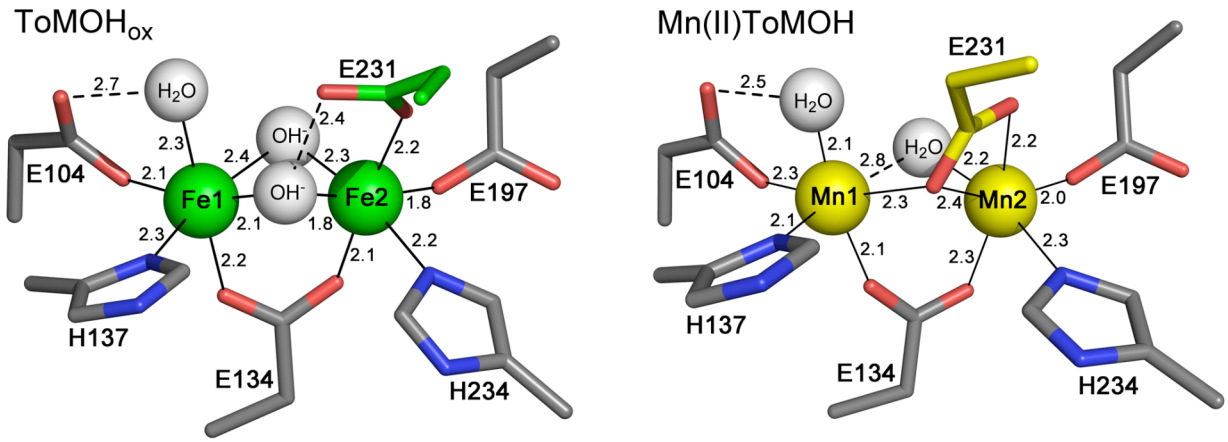

Figure S1. Active site geometries of 1.85 Å resolution ToMOH (left), and 2.20 Å resolution Mn(II)-ToMOH (right). All distances are provided in Å. Fe(III) ions, Mn(II) ions, and oxygen atom species are represented as green, yellow, and white spheres, respectively. Side chain ligands are represented as sticks in grey (carbon), red (oxygen), and blue (nitrogen).

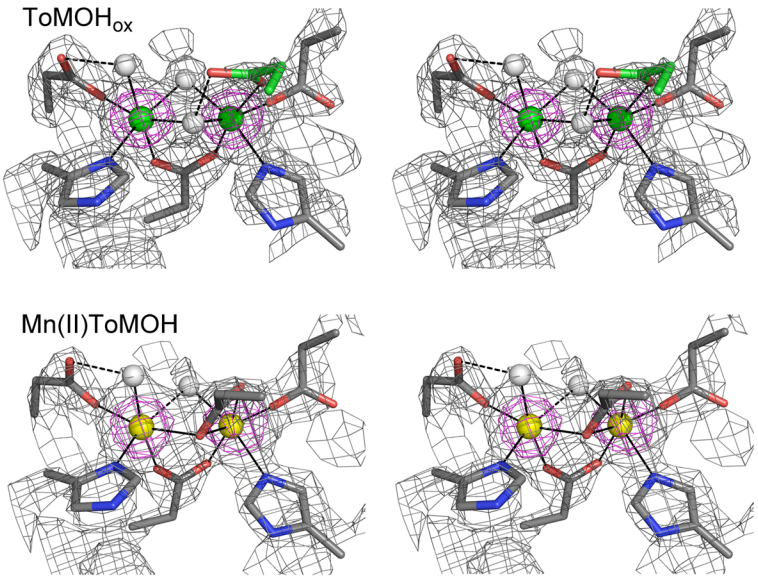

Figure S2. Active site density stereo images of 1.85 Å ToMOH$_{ox}$ (top), and 2.20 Å Mn(II)-ToMOH (bottom). Fe(III) ions, Mn(II) ions, and oxygen atoms are represented as green, yellow, and white spheres, respectively. Side chain ligands are portrayed as sticks in grey (carbon), red (oxygen), and blue (nitrogen). 2 $|F_o|$ - $|F_c|$ composite omit electron density maps contoured to 1σ and 3σ are shown in grey and magenta, respectively.

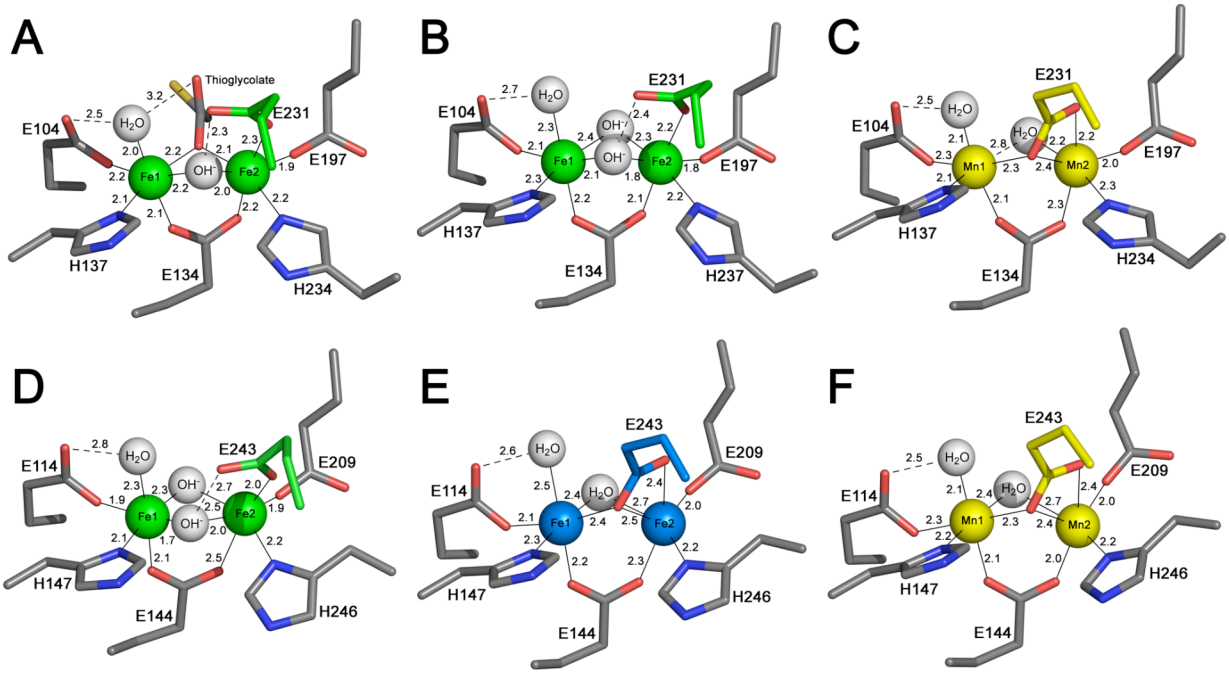

Figure S3. Active site geometries of (A) 2.15 Å $ToMOH_{ox}$ (PDB code 1T0Q), (B) 1.85 Å $ToMOH_{ox}$, (C) 2.20 Å Mn(II)-ToMOH, (D) 1.70 Å $MMOH_{ox}$ (PDB code 1MTY), (E) 2.15 Å $MMOH_{red}$ (PDB code 1FYZ), and (F) 2.30 Å Mn(II)-MMOH (PDB code 1XMF). All distances are provided in Å. Fe(III) ions, Fe(II) ions, Mn(II) ions, and oxygen atom species are represented as green, blue, yellow, and white spheres, respectively. Side chain ligands are represented as sticks in grey (carbon), red (oxygen), and blue (nitrogen).

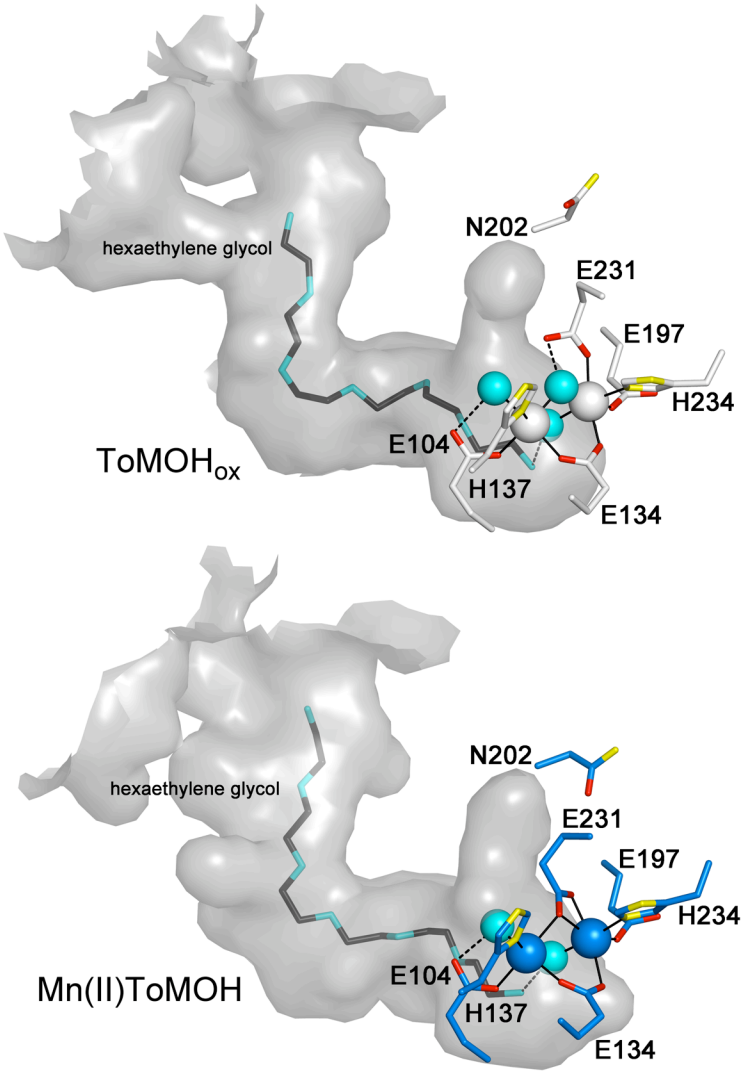

Figure S4. Hexaethylene glycol molecules modeled into the ToMOH channel in 1.85 Å ToMOH$_{ox}$ (top) and 2.20 Å Mn(II)-ToMOH (bottom). Fe(III) ions (white), Mn(II) ions (blue), and active site oxygen atom species (cyan) are represented as spheres. Hexaethylene glycol is shown as sticks in cyan (oxygen) and black (ethylene) in the channel interior. Ligating amino acid and N202 side chains are represented as sticks in white/blue (carbon), yellow (nitrogen), and red (oxygen); the protein interior van der Waals surface is shown in translucent grey.

References

(1) Sazinsky, M. H.; Bard, J.; Di Donato, A.; Lippard, S. J. *J. Biol. Chem.* **2004**, *279*, 30600-30610.

(2) Sazinsky, M. H.; Merkx, M.; Cadieux, E.; Tang, S.; Lippard, S. J. *Biochemistry* **2004**, *43*, 16263-16276.

(3) Gibbs, C. R. *Anal. Chem.* **1976**, *48*, 1197-1201.

(4) McPhillips, T. M.; McPhillips, S. E.; Chiu, H.-J.; Cohen, A. E.; Deacon, A. M.; Ellis, P. J.; Garman, E.; Gonzalez, A.; Sauter, N. K.; Phizackerley, R. P.; Soltis, S. M.; Kuhn, P. *J. Synchrotron Rad.* **2002**, *9*, 401-406.

(5) Otwinowski, Z.; Minor, W. *Method. Enzymol.* **1997**, *276*, 307-326.

(6) Brünger, A. T.; Adams, P. D.; Clore, G. M.; DeLano, W. L.; Gros, P.; Grosse-Kunstleve, R. W.; Jiang, J.-S.; Kuszewski, J.; Nilges, M.; Pannu, N. S.; Read, R. J.; Rice, L. M.; Simonson, T.; Warren, G. L. *Acta Crystallogr.* **1998**, *D54*, 905-921.

(7) McRee, D. E. *J. Struct. Biol.* **1999**, *125*, 156-165.

(8) Kissinger, C. R.; Gehlhaar, D. K.; Fogel, D. B. *Acta Crystallogr.* **1999**, *D55*, 484-491.

(9) Emsley, P.; Cowtan, K. *Acta Crystallogr.* **2004**, *D60*, 2126-2132.

(10) Murshudov, G. N.; Vagin, A. A.; Dodson, E. J. *Acta Crystallogr.* **1997**, *D53*, 240-255.

(11) Anonymous *Acta Crystallogr.* **1994**, *D50*, 760-763.

(12) Kleywegt, G. J.; Jones, T. A. *Acta. Crystallogr. D* **1998**, *54*, 1119-31.

(13) Laskowski, R. A.; MacArthur, M. W.; Moss, D. S.; Thorton, J. M. *J. Appl. Cryst.* **1993**, *26*, 283-291.